ELSEVIER

Journal of Power Sources 71 (1998) 328–336

JOURNAL OF POWER SOURCES

Numerical analyses of the internal conditions of a molten carbonate fuel cell stack: comparison of stack performances for various gas flow types

F. Yoshiba[a,*], N. Ono[b], Y. Izaki[a], T. Watanabe[a], T. Abe[c]

[a]*Chemical Energy Engineering Department, Yokosuka Research Laboratory, Central Research Institute of Electric Power Industry, 2-6-1 Nagasaka, Yokosuka, Kanagawa 240-01, Japan*

[b]*Department of Mechanical Engineering, Faculty of Engineering, Tohoku Gakuin University, 13-1 Chuo 1, Tagajyo City, Miyagi 985, Japan*

[c]*Yokosuka Research Laboratory, Central Research Institute of Electric Power Industry, 2-6-1 Nagasaka, Yokosuka, Kanagawa 240-01, Japan*

Abstract

A three-dimensional numerical analysis model of cell voltage, temperature and current profile in a molten carbonate fuel cell (MCFC) stack has been developed. 'The Formula for MCFC Performance' that was derived from the test results of a single cell having the same active components as the stack has been applied to the calculation of electrochemical performance. Calculation result of cell voltages and temperature profile showed good agreement with 10–100 kW class stack experimental data. Using this model, cell voltages, temperature profile and net output powers (MCFC output power minus required cathode recycling power) of five gas flow geometries have been compared. The calculation results showed that the net output power is highest in the co-flow geometry. From the viewpoint of a stack performance, a cooling power, and a control of maximum temperature, the co-flow type stack has advantages over the external reforming type MCFC power plant. © 1998 Elsevier Science S.A.

Keywords: Molten carbonate fuel cell; Large stack; Numerical analysis; Temperature profile

1. Introduction

Molten carbonate fuel cell (MCFC) is expected to be used in a power generation system, having high efficiency and lower emission of NO_x and SO_x. It is expected to be put into practical use as a centralized power station or dispersed power plant.

Our research group has tested not only small single cells but also 10 and 100 kW class large stacks. In those stack operating tests, we estimated the stack characteristics by measurements of each cell voltage, measurements of separator temperature, and gas composition analyses of inlet and outlet gas by gas chromatography. However, in the case of generating electricity, there are much more complicated factors such as mass and heat transfer, chemical reaction, or electrical interaction. It is very important to acquire the internal conditions of MCFC stacks by numerical models for developing cells and stacks with higher performance.

Numerical analysis of MCFC was developed in the early days by Sampath et al. [1,2]. Watanabe and colleagues analyzed the cooling characteristic of cathode gas by supposing MCFC to be a parallel heating panel [3]. Cao et al. analyzed dynamic characteristics of a single cell's temperature distribution using similar assumptions [4]. Wolf and Wilemski calculated temperature and current density distribution for co-, counter-, and cross-flow type stacks, applying the thin film cylindrical pore model to the relation between current and cell voltage (J–V characteristic). The result of the calculation showed that the best performance was achieved with counter-flow type, followed by cross- and co-flow, respectively [2]. Kobayashi, Fujimura et al. analyzed single cell and stack's temperature profile considering the mass transfer in generating reaction, and they applied the thin film cylindrical pore model to the J–V characteristic too [5,6]. However in their calculation, there was no temperature limitation of the stack.

J–V characteristic determines the heat generating rate and chemical reaction rate, so we must adhere to the J–V characteristic strictly. Concerning the J–V characteristic, our research group derived 'the Formula for MCFC Performance', which was derived from many gas and temperature conditions using small single cells having the same active component as the stack's [7,8]. Using this formulation we analyzed dynamic characteristics of the single cell [9].

Our research group measured the generating characteris-

* Corresponding author.

0378-7753/98/$19.00
PII S0378-7753(97)02727-4

tics or temperature profile of 10 kW and 100 kW class stack with 1 m^2 class large electrode area [10,11]. In these operating tests, several gas flow types of stacks have been tested, and some types of stack need large amounts of cooling gas. We had developed a 2-dimensional analysis model for the co-flow type stack [12]. However there are many different types of stack, such as counter, cathode exchange parallel, cross and cathode exchange crossflow. In this paper a 3-dimensional temperature and current density analysis model is developed, that appies the 'Formulation for MCFC Performance' derived from a 100-cm^2 single cell test having the same active component as those of the stack. Stack performances and cooling gas flow rates with five gas flow types are compared under the MCFC's normal operating conditions.

1.1. Variables and subscripts

Variables

C	mol concentration (mol/m^3)
C_p	specific heat at constant pressure (J/kg·K)
E	electromotive force (V)
F	Faraday constant (C/mol)
h	coefficient of heat tansfer (W/m^2·K)
I	load current (A)
J	current density (A/m^2)
K_p	equilibrium constant
L	gas channel length (m)
m	molar fraction (–)
M	molar weight (kg/mol)
P	partial pressure (Pa)
q	heat flow rate (W/m^2)
q_{GEN}	heating value of generating reaction (W/m^2)
q_{SHIFT}	heating value of shift reaction (W/m^2)
R_{ir}	internal resistance (Ω·m^2)
R_a	anode reaction resistance (Ω·m^2)
R_c	cathode reaction resistance (Ω·m^2)
R_s	electrical resistance of separator (Ω)
r_{GEN}	generating reaction rate (mol/m^2·S)
r_{SHIFT}	shift reaction rate (mol/m^3·S)
T	temperature (K)
u	gas velocity (m/s)
V	cell voltage (V)
Y	cell width (m)
α_{GEN}	formation enthalpy of H_2O (J/kg)
α_{SHIFT}	enthalpy of shift reaction (J/kg)
δ	thickness of channel and each component (m)
ϵ	thickness of corrugated plate (m)
σ	Stefan-Boltzmann constant (W/m^2·K^4)
λ	heat conductivity (W/m·K)
τ	anode gas residence time in anode channel (s)

Subscripts

a	anode
c	cathode
e	electrolyte and electrode
s	separator
w	corrugated plate

Subscript of a gas such as H_2, CO_2, etc. means each kind of gas, and two continuous subscripts refers to the relation between each component.

2. Modeling of the system and governing equations

2.1. Modeling of the system

A single cell's structure of MCFC is shown in upper part of Fig. 1. The single cell is constructed by separator plates, corrugated plates, current collectors, electrodes (cathode and anode), and electrolyte. Fuel and oxidant gas flow in anode and cathode side channel along the corrugated plates. O_2 and CO_2 in oxidant gas react with electron at the cathode, and produce CO_3^{2-}. CO_3^{2-} moves within the electrolyte plate perpendicularly from cathode to anode by the driving force of concentration difference. In the anode, H_2 in fuel gas reacts with CO_3^{2-} and produces CO_2, H_2O and electrons by electro-chemical reaction. Electrons released from the reaction site are collected by the current collector and pass the corrugated plate and separator perpendicularly. The top and bottom separators are connected to loading equipment.

The heat produced within the electric generating reaction is transferred to each gas by convection and with mass transfer, to the separator by radiation directly and by heat conduction through the corrugated plate. We simplified the model, which is schematized in the lower part of Fig. 1. Here we put electrolyte, electrode and current corrector together as one component.

2.2. Approximation and governing equations

We applied assumption and approximation as follows to derive basic equations.

1. Cell voltage has no distribution in the cell plain.
2. Density and characteristic value of anode and cathode gas are a function only of the gas composition.
3. Heat conduction by each gas and electrolyte plates are negligible.

Mass balance. Mole flow changing rates of each gas and mixed gas for cell no. j are written as follows.

Cathode gas:

$$\delta_c \cdot \frac{dC_{c,k} \cdot u_c}{dx} = A \cdot r_{GEN}$$

$$C_c \cdot \delta_c \cdot \frac{du_c}{dx} = -\frac{3}{2} r_{GEN} \quad (1)$$

where k denotes each gas composition, CO_2, O_2, N_2 coefficient A denotes −1 for CO_2, −1/2 for O_2, 0 for N_2, respectively. In the case of analyzing the cross-flow type stack, the derivative term is applied for the y-direction.

Anode gas:

$$\delta_a \cdot \frac{dC_{a,l} \cdot u_a}{dx} = B \cdot r_{GEN} + C \cdot \delta_a \cdot r_{SHIFT}$$

$$C_a \cdot \delta_a \cdot \frac{du_a}{dx} = r_{GEN} \quad (2)$$

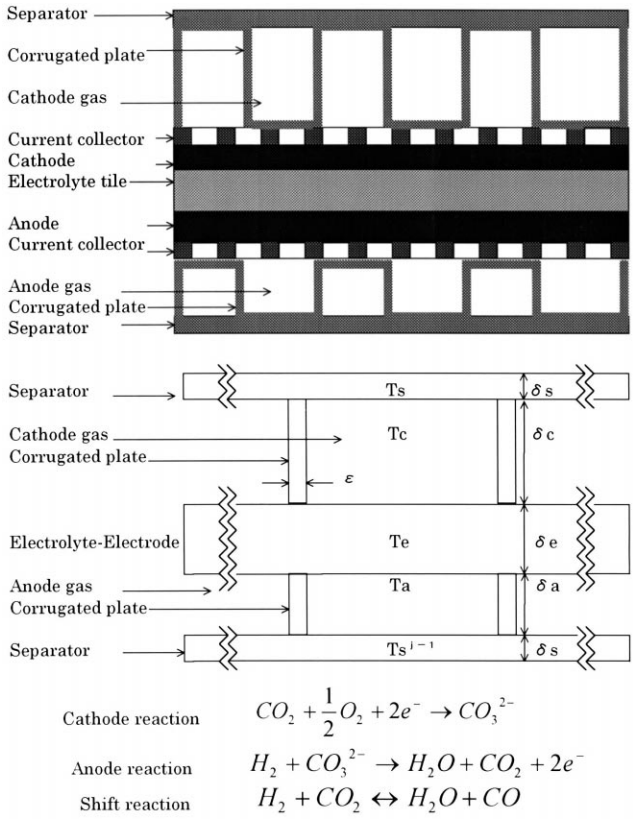

Fig. 1. Conceptual structure of single cell and analysis model.

where l denotes each gas composition, H_2, CO_2, H_2O, CO, coefficient B denotes −1 for H_2, 1 for CO_2 and H_2O, 0 for CO and coefficient C denotes 1 for H_2 and CO_2, −1 for H_2O and CO, respectively.

Generating reaction rate is expressed as follows.

$$r_{\mathrm{GEN}} = \frac{J(x,y)}{2 \cdot F} \tag{3}$$

Equation of shift reaction in the anode gas is expressed as follows.

$$\frac{1}{K_{\mathrm{p}}(T_a)} = \frac{(C_{\mathrm{H_2}} + X) \cdot (C_{\mathrm{CO_2}} + X)}{(C_{\mathrm{H_2O}} - X) \cdot (C_{\mathrm{CO}} - X)} \tag{4}$$

Where X denotes concentration change rate of shift reaction. As is known, residence time is short in the case where mesh width for x-direction is short, so the shift reaction could not be at equilibrium as in Eq. (4). In this calculation we expressed shift reaction rate as follows, using adjusted coefficient parameter α (<1).

$$r_{\mathrm{SHIFT}} = \alpha \cdot \frac{X}{\tau} = \alpha \cdot X \cdot \frac{u_{\mathrm{a}}}{\Delta x} \tag{5}$$

Energy equation. Energy conservation equations of cell no. j are written as follows; here subscript $j-1$ and $j+1$ denote adjoining cell number.

Cathode gas:

$$\delta_{\mathrm{c}} \cdot \sum_k \left(\frac{\mathrm{d}\rho_k \cdot Cp_k \cdot u_{\mathrm{c}} \cdot T_{\mathrm{c}}}{\mathrm{d}x} \right) = q_{\mathrm{sc}} + q_{\mathrm{ec}} + q_{\mathrm{wc}} - q_{\mathrm{GENec}} \tag{6}$$

where k denotes gas composition CO_2, O_2, N_2. In the case of analyzing the cross-flow type stack, the derivative term is applied for the y-direction.

Anode gas:

$$\delta_{\mathrm{a}} \cdot \sum_l \left(\frac{\mathrm{d}\rho_l \cdot Cp_l \cdot u_{\mathrm{a}} \cdot T_{\mathrm{a}}}{\mathrm{d}x} \right) = q_{\mathrm{sa}}^{j-1} + q_{\mathrm{ea}} + q_{\mathrm{wa}} - q_{\mathrm{GENea}} + q_{\mathrm{SHIFT}} \tag{7}$$

where l denotes H_2, CO_2, H_2O, CO.

Electrolyte with electrode plate:

$$q_{\mathrm{GEN}} - q_{\mathrm{ec}} - q_{\mathrm{ea}} - q_{\mathrm{es}} - q_{\mathrm{es}}^{j-1} - q_{\mathrm{ew}} - q_{\mathrm{ew}}^{j-1} + q_{\mathrm{GENec}} + q_{\mathrm{GENea}} = 0 \tag{8}$$

Separator plate:

$$-\lambda_{\mathrm{s}} \cdot \delta_{\mathrm{s}} \cdot \left(\frac{\partial^2 T_{\mathrm{s}}}{\partial x^2} + \frac{\partial^2 T_{\mathrm{s}}}{\partial y^2} \right) = q_{\mathrm{se}} + q_{\mathrm{se}}^{j+1} + q_{\mathrm{sw}} + q_{\mathrm{sw}}^{j+1} - q_{\mathrm{sc}} - q_{\mathrm{sa}}^{j+1} \tag{9}$$

Convection heat transfer term in energy equation is expressed as follows.

$$q_{\mathrm{sc}} = h_{\mathrm{sc}} \cdot (T_{\mathrm{s}} - T_{\mathrm{c}}) \quad q_{\mathrm{ec}} = h_{\mathrm{ec}} \cdot (T_{\mathrm{e}} - T_{\mathrm{c}})$$

$$q_{\mathrm{sa}} = h_{\mathrm{sa}} \cdot (T_{\mathrm{s}} - T_{\mathrm{a}}) \quad q_{\mathrm{ea}} = h_{\mathrm{ea}} \cdot (T_{\mathrm{e}} - T_{\mathrm{a}}) \tag{10}$$

where heat transfer coefficient is expressed as $h = N \cdot \lambda/\delta$, and in this analysis, we selected $Nu = 3.0$. Radiation term from electrolyte plate to separator plate is expressed and approximated as follows.

Cathode side:

$$q_{\mathrm{es}} = \sigma \cdot \phi_{\mathrm{c}} \cdot (T_{\mathrm{e}}^4 - T_{\mathrm{s}}^4) \approx 4 \cdot \sigma \cdot \phi_{\mathrm{c}} \cdot T^{*3} \cdot (T_{\mathrm{e}} - T_{\mathrm{s}})$$

Anode side:

$$q_{\mathrm{es}} = \sigma \cdot \phi_{\mathrm{a}} \cdot (T_{\mathrm{e}}^4 - T_{\mathrm{s}}^4) \approx 4 \cdot \sigma \cdot \phi_{\mathrm{a}} \cdot T^{*3} \cdot (T_{\mathrm{e}} - T_{\mathrm{s}}) \tag{11}$$

where ϕ_{c}, ϕ_{a} are the geometric factor in each gas channel, and T^* represents a temperature of 923 K (650°C).

Concerning heat conduction by corrugated plate and convection heat transfer from corrugated plate to each gas, we proposed a heat transfer model and calculated heat transfer by exact solution.

$$\epsilon \cdot \lambda \frac{\partial^2 T(z)}{\partial z^2} - 2 \cdot h_{\mathrm{wc}} \cdot \{T(z) - T_c\} = 0 \tag{12}$$

where z is the coordinate for stacking direction.

Heat generation by generating and shift reaction is expressed as follows.

$$q_{\mathrm{GEN}} = \alpha_{\mathrm{GEN}} \cdot r_{\mathrm{GEN}} \quad q_{\mathrm{SHIFT}} = \alpha_{\mathrm{SHIFT}} \cdot r_{\mathrm{SHIFT}} \tag{13}$$

Heat transfer by gas enthalpy with generation reaction is written as follows.

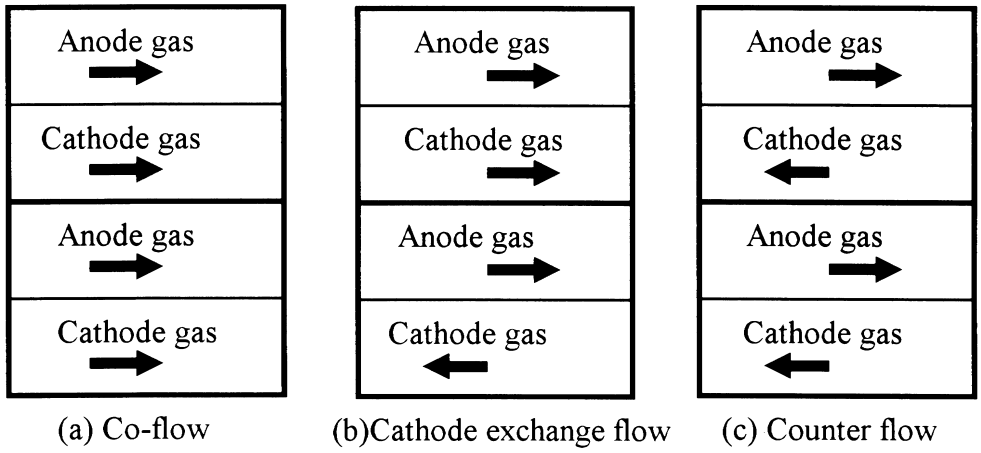

Fig. 2. Conceptual gas flow design of three parallel flow type stacks.

$$q_{\mathrm{GENea}} = (Cp_{\mathrm{H_2}} \cdot M_{\mathrm{H_2}} \cdot T_{\mathrm{a}} - Cp_{\mathrm{CO_2}} \cdot M_{\mathrm{CO_2}} \cdot T_e - Cp_{\mathrm{H_2O}} \cdot T_{\mathrm{e}}) \cdot r_{\mathrm{GEN}}$$

$$q_{\mathrm{GENec}} = \left(Cp_{\mathrm{CO_2}} \cdot M_{\mathrm{CO_2}} \cdot T_{\mathrm{c}} + \frac{1}{2} \cdot Cp_{\mathrm{O_2}} \cdot M_{\mathrm{O_2}} \cdot T_{\mathrm{c}}\right) \cdot r_{\mathrm{GEN}} \quad (14)$$

Current density profile and output power voltage. In ordinary MCFC's operating condition, the relation between cell voltage and current density is written as follows.

$$V \cong E(x,y) - \{R_{\mathrm{ir}}(x,y) + R_{\mathrm{a}}(x,y) + R_{\mathrm{c}}(x,y)\} \cdot J(x,y) = E(x,y) - R_{\mathrm{p}}(x,y) \cdot J(x,y) \quad (15)$$

Nernst voltage and cell resistance is written as follows [7,8,13].

$$E = E^0 + \frac{RT_{\mathrm{e}}}{2 \cdot F} \ln \frac{P_{\mathrm{H_2a}} \cdot P_{\mathrm{CO_2c}} \cdot P_{\mathrm{O_2c}}^{1/2}}{P_{\mathrm{CO_2a}} \cdot P_{\mathrm{H_2Oa}}} \quad (16)$$

$$R_{\mathrm{ir}} = AR \cdot \exp\left(-\frac{\Delta HR}{R \cdot T_{\mathrm{e}}}\right) \quad (17)$$

$$R_{\mathrm{a}} = AR_{\mathrm{an}} \cdot T_{\mathrm{e}} \cdot \exp\left(-\frac{\Delta H_{\mathrm{a}}}{R \cdot T_{\mathrm{e}}}\right) \cdot P_{\mathrm{H_2a}}^{-0.5} \quad (18)$$

$$R_{\mathrm{c}} = A_{\mathrm{D}} \cdot T_{\mathrm{e}} \cdot \exp\left(-\frac{\Delta H_{\mathrm{O_2}}}{R \cdot T_{\mathrm{e}}}\right) \cdot P_{\mathrm{O_2}}^{-0.75} \cdot P_{\mathrm{CO_2}}^{0.5} + A_{\mathrm{E}} \cdot T_{\mathrm{e}} \cdot \exp\left(-\frac{\Delta H_{\mathrm{CO_2}}}{R \cdot T_{\mathrm{e}}}\right) \cdot m_{\mathrm{CO_2}}^{-1.0} \quad (19)$$

where AR, ΔHR denote the frequency coefficient of

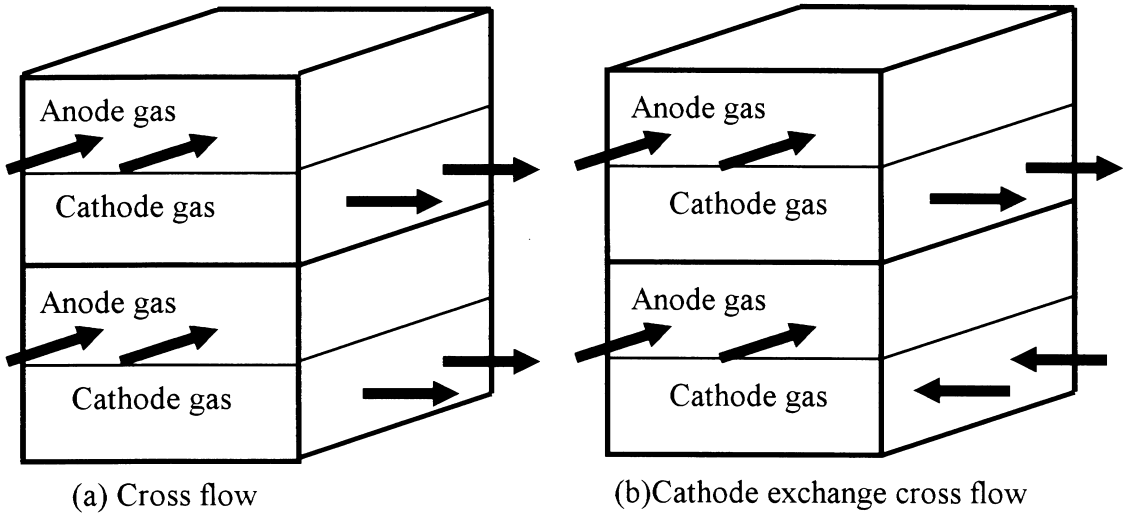

Fig. 3. Conceptual gas flow design of two cross-flow type stacks.

Table 1

Characteristic value and cell size

Legends	Values (unit)
λ_s	22.0 (W/m^{2}K)
h_{sa}, h_{ea}, h_{wa}	593.1 (W/m^{2}K)
hsa, h_{ea}, h_{wc}	91.1 (W/m^{2}K)
ϕ_c	0.43 (–)
ϕ_a	0.25 (–)
Rs	2.5×10^{-6} (Ω)
δa	1.0×10^{-3} (m)
δc	2.0×10^{-3} (m)
Lx	1.0 (m)
Ly	1.0 (m)

internal resistance and activation energy, respectively. ΔH_a, ΔH_{O_2}, ΔH_{CO_2} are activation energy of each gas, AR_{an}, A_D, A_E are the coefficients that have been derived from test result of a single cell.

In the constant cell voltage over the cell plain, the next equation is derived from Eq. (15) as follows.

$$V = \left\{ \int_0^{dy} \int_0^{dx} \frac{E(x,y)}{Rp(x,y)} dx \cdot dy - I \right\} \Big/ \int_0^{dy} \int_0^{dx} \frac{1}{Rp(x,y)} dx dy \quad (20)$$

Using mass equations Eqs. (1) and (2), energy equations Eqs. (6)–(9), and current and voltage Eq. (20), we can calculate the temperature profile, gas concentration profile, and current density profile of each cell in the stack.

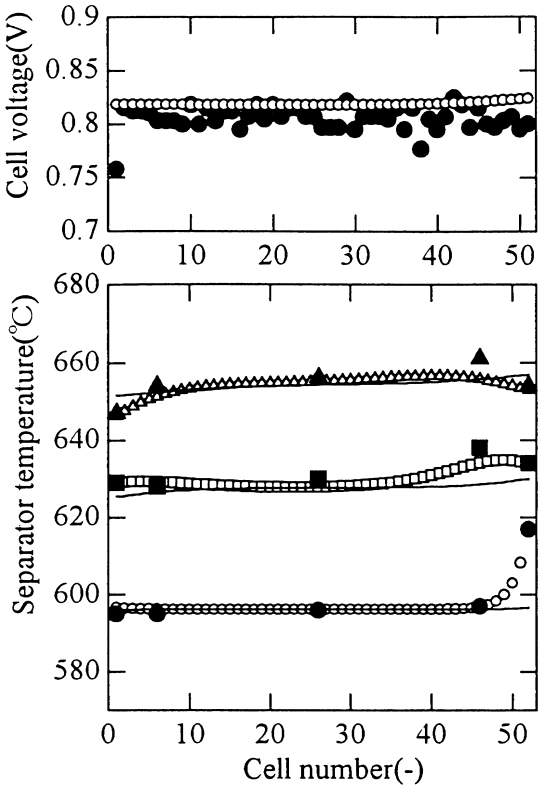

Fig. 4. Comparison of calculated cell voltage and separator temperature profile for co-flow type stack. Operating pressure: 0.49 MPa; current density: 1500 A/m^2; fuel utilization: 80%; overall oxidant utilization: 30%; cathode recycling ratio: 62%; cell voltage: (●) Experimental, (○) Calculated. Temperature experimental: (●) anode inlet, (■) center of cell, (▲) anode outlet. Temperature calculated: (○) anode inlet, (□) center of cell, (△) anode outlet. Line calculated under the adiabatic condition.

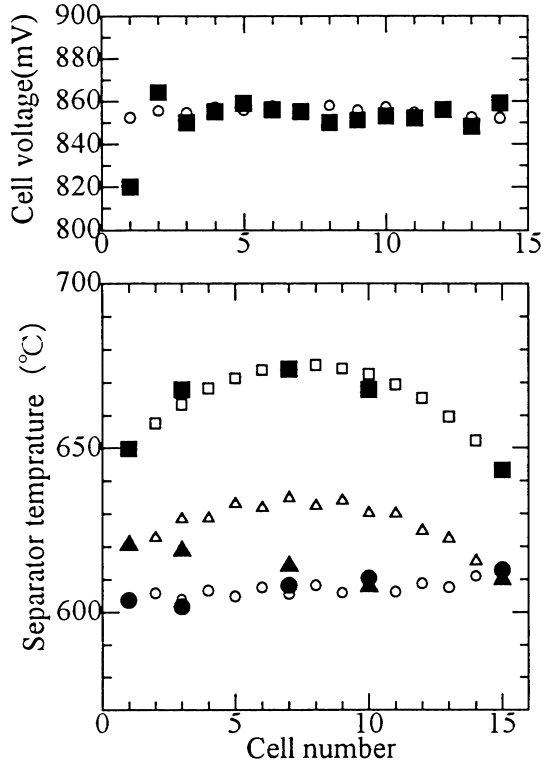

Fig. 5. Comparison of calculated separator temperature with experimental data. Operating pressure: 0.49 MPa; current density: 1500 A/m^2; fuel utilization: 60%; overall oxidant utilization: 30%; Cathode recycling ratio: 72%; Cell voltage: (■) Experimental, (○) Calculated. Temperature experimental: (●) anode inlet, (■) center of cell, (▲) anode outlet. Temperature calculated: (○) anode inlet, (□) center of cell, (△) anode outlet.

2.3. Gas flow configuration of several types of stack

We calculate the stack performance and temperature profile for various gas flow types as shown in a later section. Figs. 2 and 3 show the conceptual configuration of every gas flow type. In all types, anode gas flows in only one direction. In the co-flow type, cathode gas flows in the same direction as anode gas, while in counter-

Table 2

Coefficient of cell performance

	Value	Unit
AR	1.27×10^{-2}	
ΔHR	-27.9×10^3	J/mol
AR_{an}	8.11×10^{-9}	
ΔH_a	-109.6×10^3	J/mol
A_D	2.24×10^{-9}	
ΔH_{O_2}	-82.8×10^3	J/mol
A_E	1.51×10^{-6}	
ΔH_{CO_2}	-26.9×10^3	J/mol

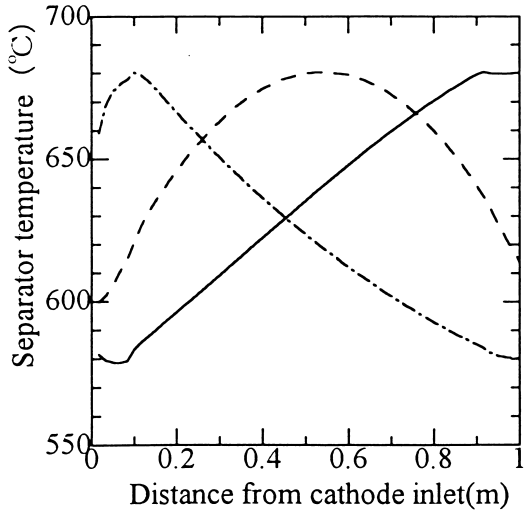

Fig. 6. Seperator temperature profile for three types of parallel flow type stack. ——— Co-flow; - - - cathode exchange flow; – · – counter-flow. Operating pressure: 0.49 MPa; current density: 2000 A/m^2; fuel utilization: 80%; overall oxidant utilization: 30%; maximum separator temperature: 680°C.

flow type it flows in the opposite direction, and in cathode exchange the flow is a combination of co-flow and counter-flow. In cross-flow, the cathode gas flows in a perpendicular direction, and every cathode flows in the opposite direction in the cathode exchange cross-flow.

2.4. Numerical analysis method and calculating conditions

In numerical analysis, we applied successive difference approximation for first the derivative term of mass equation and secondary successive difference approximation for the energy equation, and center difference approximation for second derivative term. To calculate temperature profile

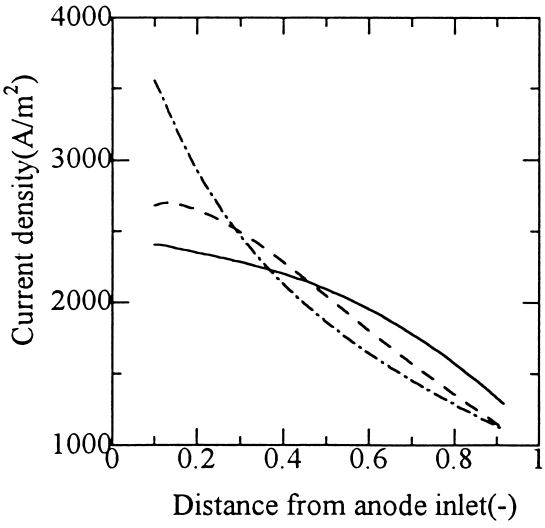

Fig. 7. Current density for three types of parallel flow. – · – Co-flow; - - - cathode exchange flow; ——— counter-flow.

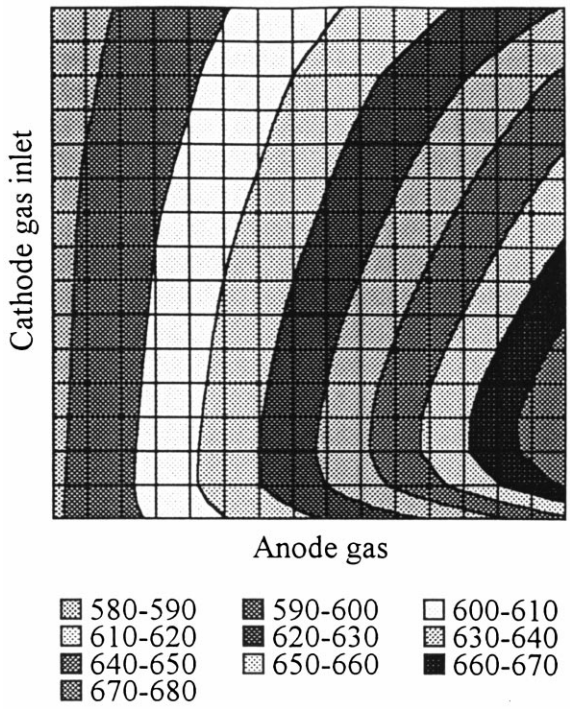

Fig. 8. Temperature distribution of cross-flow type stack.

we made a large matrix and calculated using the successive over relaxation (SOR) method. Table 1 shows characteristic values and cell size. For the coefficient of 'Formula for MCFC Performance' that was derived from a single cell having the same active component as the stack, we used parameters as shown in Table 2.

From investigation of accuracy, a mesh width of 10 mm

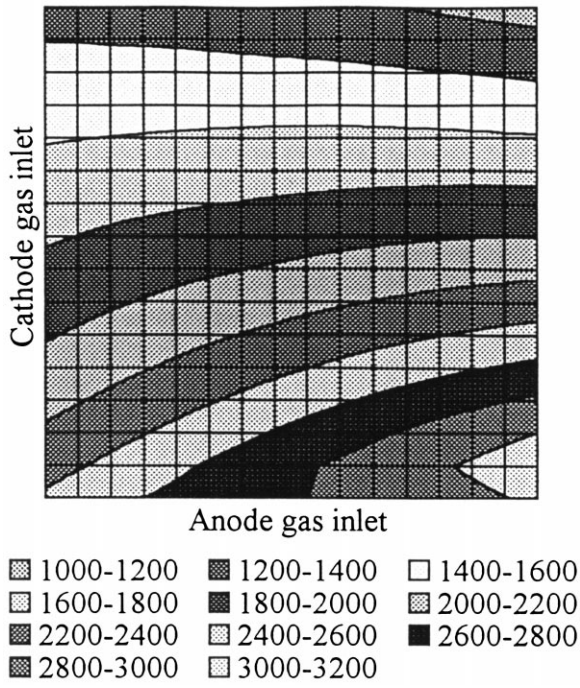

Fig. 9. Current density distribution of cross-flow type stack.

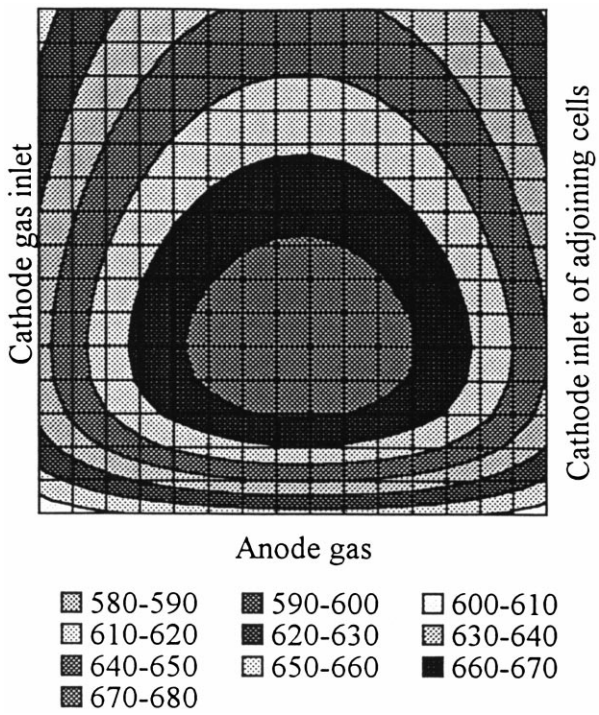

Fig. 10. Temperature distribution of cathode exchange cross-flow.

was selected. From the result of a single cell test, shift reaction becomes equivalent in less than 1 s, but the reaction time is not clear, so we selected $\alpha = 0.25$ to delay the shift reaction.

3. Results and discussion

3.1. Comparison with experimental results

3.1.1. Analysis of co-flow type stack

Fig. 4 compares calculated data with experimental data of each cell voltage and temperature profile within a 100 kW class stack's lower module consisting of 51 cells. The gas flow type is co-flow, and the cathode recycling ratio was calculated from the measurement of cathode inlet and outlet gas composition analysis using gas chromatography. Each calculated cell voltage shows good agreement with experimental data except the low voltage cell. Calculated temperature profile also shows good agreement with experimental data. These results proved that the constructed model is valid as the stack's internal condition analysis method. Temperature profile in the figure was calculated under the assumption of adiabatic conditions at the end separators. Good agreement of the calculated temperature with the test result means that the stack was operated under adiabatic conditions at end separators.

3.1.2. Analysis of cathode exchange parallel flow type stack

Fig. 5 (upper) compares calculated data with measured cell voltage for cathode exchange parallel flow type 10 kW class stack. The stack consisted of 14 cells, and each calculated cell voltage had good agreement with those observed, except cell no. 1. The calculated cell voltage of even-numbered cells are higher than odd-numbered cells, since both anode and cathode gas flows in the same direction in even-numbered cells and in the opposite direction in odd-numbered cells.

Fig. 5 (lower) shows the comparison for calculated temperature profile in the center of the gas flow channel with experimental data. The calculated result shows good agreement with the experimental data except for the anode outlet side. The difference between calculated data and experimental data for the anode outlet side seems to be caused by the heat loss on the outside of the stack. Since hot cathode outlet gas heat exchanges with cold cathode inlet gas of the adjoining cell, the maximum temperature is observed at the center of the stack. Therefore the average temperature is higher than for the co-flow type stack discussed before, so the cell voltage is also better.

From the comparison of experimental data for the co-flow and cathode exchange parallel flow type stack, our analysis model is useful for temperature analysis of the MCFC stack.

3.2. Analysis of other gas flow type stacks

Using the model that we developed, we calculated the temperature and current density profile for various gas flow type stacks. The calculated gas flow types are three types of parallel flow and two types of cross-flow, shown in Figs. 2 and 3.

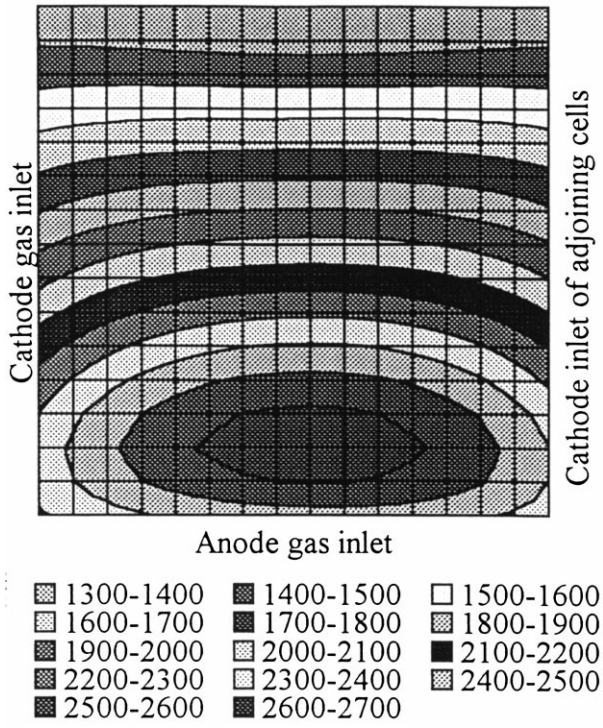

Fig. 11. Current density of cathode exchange cross-flow.

Table 3

Comparison of stack performances about various gas flow types

	Parallel flow type			Cross-flow type	
	Co-flow	Counter-flow	Cathode exchange	Cross	Cathode exchange
Cell voltage (mV)	780	783	**793**	768	**793**
Cathode recycling ratio (%)	**39**	56	76	62	81
Cathode outlet temperature (°C)	**680**	670	620	656	625

Calculation conditions are as follows. Operating pressure: 0.49 MPa; current density: 2000 A/m^2; fuel utilization: 80%; overall oxidants utilization: 30%; cathode gas inlet temperature: 580°C; maximum seperator temperature: 680°C. Adiabatic conditions at separator edge and end separator, and the gas flow distribution in the cell plane is uniform.

3.2.1. Calculations for parallel flow

Figs. 6 and 7 show the calculated temperature profile and current density profile for three parallel flow type stacks. The maximum cell voltage was observed in the cathode exchange flow (793 mV), followed by counter-flow (783 mV) and co-flow (780 mV), respectively. However in the cathode exchange parallel flow and counter-flow type stack, the cathode recycling ratio is too much to keep the maximum temperature 680°C, and the stack's maximum temperature position is in the generating area. In the co-flow type stack the maximum temperature of the stack is located at the cathode outlet side, so the outlet gas temperature is the same as the stack's maximum temperature, which means the co-flow type has an advantage in observing the maximum stack temperature. In the counter-flow type, since much of the steam that is generated by the generating reaction is supplied for the minimum temperature point, located at the anode outlet side, the type has an advantage from the viewpoint of carbon deposition.

3.2.2. Calculations for cross-flow

In this paper we developed a three-dimensional analysis model, which can analyze the cross-flow type stack. Figs. 8–11 show temperature and current density distribution for two cross-flow type stacks, cross and cathode exchange cross-flow. Supposed operating conditions are the same as the parallel flow case. Both maximum temperature and current density of the cross-flow are located at the anode inlet and cathode outlet side, since anode gas has fresh composition and cathode gas is hot in that area. In the cathode exchange cross-flow type stack, the maximum temperature is located at the center of the cell, and maximum current density is located at the center of anode inlet side. To calculate the cathode outlet temperature, we must integrate all of the outlet gas channel because the gas temperature is different at all points, while parallel flow needs no integration. The calculated cathode outlet gas temperature is 655°C in cross-flow and 625°C in cathode exchange cross-flow.

Table 4

Calculation conditions of cathode recycling blower consumption

Adiabatic efficiency	80%
Electric motor efficiency	95%
Inlet pressure	0.49 MPa
Outlet pressure	0.54 MPa
Inlet gas temperature	680°C (co-flow)
	620°C (cathode exchange parallel flow)
	670°C (counter-flow)

3.3. Comparison of net output power from the stack

From the viewpoint of high efficiency generation of MCFC plant, calculation of net output power from the stack is important, considering the maximum temperature and cathode recycling blower consumption. Table 3 shows the stack output power, cathode recycling ratio and cathode outlet temperature for three types of parallel flow and two types of cross-flow. The calculated conditions are 580°C cathode inlet and 680°C maximum separator temperature. The gas flow type which shows higher output voltage, lower cathode recycling ratio, and higher cathode outlet temperature has advantages for the external reforming MCFC plant. From the result, two types of cathode exchange flow show higher output voltage; co-flow shows minimum cathode recycling ratio and maximum cathode outlet temperature.

Even if the output cell voltage is higher, much cathode

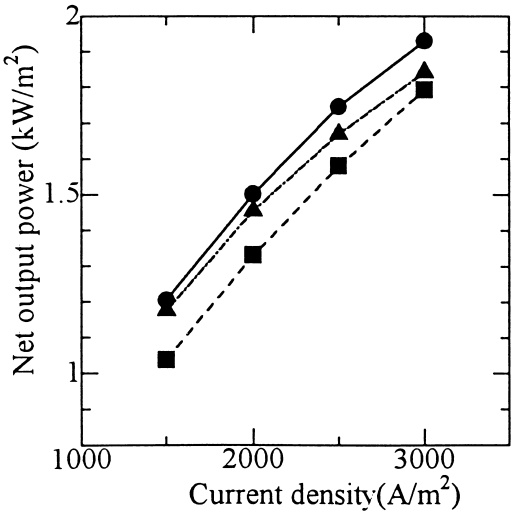

Fig. 12. Net output power of MCFC stack. Net output power is MCFC output minus required cathode blower power. Operating pressure: 0.49 MPa; fuel utilization: 80%; overall oxidant utilization: 30%; maximum separator temperature: 680°C; cathode inlet temperature: 580°C. (●) Co-flow; (■) cathode exchange flow; (▲) counter-flow.

recycling power makes the net output lower. To estimate the net output power from the stack, we calculated the cathode recycling blower consumption of three parallel flow types under the conditions shown in Table 4.

Fig. 12 shows the net output power density vs. operating current density. In the figure, net output power means MCFC output power density minus cathode recycling blower consumption. From lower current density to higher current density operating conditions, the co-flow type stack shows the highest net output power density even if the cell voltage is not so good, since co-flow type's cathode recycling consumption is the lowest. Furthermore in Table 4 the cross-flow type stack's net performance is lower than co-flow, since cell voltage is lower and the cathode recycling rate is higher, and cathode exchange cross-flow is lower than cathode exchange parallel flow because the cathode recycling rate is higher even if the cell voltage is high.

4. Conclusions

We developed a three-dimensional numerical analysis model that can calculate temperature profile, current profile, and each cell voltage for an MCFC stack with five gas flow types. Good agreement of each calculated cell voltage and temperature profile with experimental data of two gas flow type stacks showed that the model we constructed is valid for MCFC stack internal conditions analysis.

Using the model, we analyzed five gas flow type stack performances. Results showed that in the case of uniform gas distribution in the cell plane, the co-flow type stack showed the highest net output power with the assumption of maximum temperature limitation. Moreover in the co-flow type stack, the temperature of cathode outlet gas is almost equivalent to the maximum temperature of the stack, so it is easier for observing the maximum temperature of the stack. From the viewpoint of stack performance, cooling power, and control of maximum temperature, the co-flow type stack is the most advantageous.

Acknowledgements

A part of the experimental results and stack geometry in this paper were obtained in joint research with Hitachi, Ltd., and with Ishikawajima-Harima Heavy Industry Co., Ltd. The authors thank co-workers in these companies for the kind advice and the opportunity to operate their stacks.

References

[1] V. Sampath, A.F. Sammells and J.R. Selman, *J. Electrochem. Soc., 127 (1)* (1980) 79.
[2] T.L. Wolf and G. Wilemski, *J. Electrochem. Soc., 130 (1)* (1983) 49.
[3] T. Watanabe and I. Nikai, *JSME B, 52 (481)*, (1986) 3335.
[4] G. Cao and M. Masubuchi, *JSME B, 57 (535)* (1991) 837.
[5] N. Kobayashi, H. Fujimura and K. Ohtsuka, *JSME B, 54 (505)* (1988) 2568.
[6] H. Fujimura, N. Kobayashi and K. Ohtsuka, *JSME B, 57 (535)* (1991) 825.
[7] Y. Mugikura, T. Abe, T. Watanebe and Y. Izaki, *Denki Kagaku, 60 (2)* (1992) 124.
[8] H. Morita, Y. Magikura and Y. Izaki, *Denki Kagaku, 63 (11)* (1995) 1053.
[9] T. Watanebe, E. Koda, E. Mugikura and Y. Izaki, *Denki Kagaku, 60 (2)* (1992) 124.
[10] E. Mugikura, Y. Izaki, T. Watanebe, T. Abe, T. Shimizu, S. Sato and T. Matsuyama, *Evaluation of a 10 kW Class MCFC Stack Performance by a Correlation Equation*, CRIEPI Report W93020, 1994.
[11] Y. Izaki, T. Watanabe, T. Abe, M. Tooi, T. Matsuyama and M. Hosaka, *JSME B, 61 (592)* (1995) 12.
[12] F. Yoshiba, T. Abe, C. Guangyi and T. Watanabe, *JSME B, 63 (606)* (1997) 2.
[13] H. Morita, Y. Mugikura. Y. Izaki, T. Watanabe and T. Abe, in *The 3rd FCDIC Fuel Cell Symposium Proceedings*, June, 1996, pp. 173–178.